



Electrochemical properties of Cu₆Sn₅ alloy powders directly prepared by spray pyrolysis

Seo Hee Ju, Hee Chan Jang, Yun Chan Kang*

Department of Chemical Engineering, Konkuk University, 1 Hwayang-dong, Gwangjin-gu, Seoul 143-701, Republic of Korea

ARTICLE INFO

Article history:

Received 2 July 2008

Received in revised form 1 October 2008

Accepted 1 October 2008

Available online 17 October 2008

Keywords:

Alloy powder

Anode materials

Spray pyrolysis

Lithium secondary battery

ABSTRACT

Spherical shape Cu–Sn alloy powders with fine size for lithium secondary battery were directly prepared by spray pyrolysis. The mean size and geometric standard deviation of the Cu–Sn alloy powders prepared at a temperature of 1100 °C were 0.8 μm and 1.2, respectively. The powders prepared at a temperature of 1100 °C with low flow rate of carrier gas as 5 l min⁻¹ had main XRD peaks of Cu₆Sn₅ alloy and copper-rich Cu₃Sn alloy phases. Cu and Sn components were well dispersed inside the submicron-sized alloy powders. The discharge capacities of the Cu₆Sn₅ alloy powders prepared at a flow rate of 5 l min⁻¹ dropped from 485 to 313 mAh g⁻¹ by the 20th cycle at a current density of 0.1 C. On the other hand, the discharge capacities of the Cu–Sn alloy powder prepared at a flow rate of 20 l min⁻¹ dropped from 498 to 169 mAh g⁻¹ by the 20th cycle at a current density of 0.1 C.

© 2008 Elsevier B.V. All rights reserved.

1. Introduction

Many types of materials including alloy powders are studied as the electrode materials with high capacity for lithium ion batteries. Tin-based powders have been widely studied because of its high specific gravimetric capacity (about 990 mAh g⁻¹) and volumetric capacity (about 7200 mAh cm⁻³) [1,2]. However, the poor cycleability due to large volume change (up to 360%) during cycling makes it impractical to use pure tin metal as electrode for rechargeable lithium ion batteries [3]. To overcome this problem, tin-based intermetallic compounds Sn_xM_y (M: inactive material) have been reported as promising electrode materials, including Cu–Sn, Ni–Sn, Sb–Sn and Fe–Sn systems [4–9]. Among these alloys, the Cu–Sn alloy is one of the most promising anodes of lithium ion batteries because of its low price, high conductivity, and good retention of capacity. In preparation of Cu–Sn alloy powders, various preparation techniques including high-energy ball milling, chemical reduction in aqueous solution and non-aqueous solution, and solid-state reaction have been studied [10–13].

Spray pyrolysis is thought to be an effective technique to prepare the alloy powders for short production time and homogeneous composition. The alloy powders prepared by spray pyrolysis had spherical shape, narrow size distribution, fine size, homogeneous

composition and dense structure. Spray pyrolysis was applied to the preparation of pure metal and alloy powders. The pure metal and alloy powders for displays and multilayer ceramic capacitors (MLCCs) were mainly studied in the spray pyrolysis [14,15]. The electrochemical properties of the alloy powders directly prepared by spray pyrolysis were not well studied.

In this work, spherical shaped Cu–Sn alloy powders were directly prepared by spray pyrolysis under reducing atmosphere (H₂/N₂ = 10%/90%). The effects of preparation conditions on the morphological and electrochemical properties of the alloy powders were investigated.

2. Experimental

The spray pyrolysis system consists of a droplet generator, a quartz reactor, and a powder collector. A 1.7-MHz ultrasonic spray generator with six vibrators was used to generate a large quantity of droplets, which were carried into the high-temperature tubular reactor by a carrier gas. The flow rates of reducing gas (H₂/N₂ = 10%/90%) used as carrier gas were 5 and 20 l min⁻¹. The droplets and powders evaporated, decomposed, and/or crystallized in the quartz reactor. The length and diameter of the quartz reactor are 1000 mm and 50 mm, respectively. The reactor temperature was fixed at 1100 °C. The spray solution was prepared by dissolving a stoichiometric ratio of copper nitrate hydrate [Cu(NO₃)₂·3H₂O, Aldrich] and stannic chloride hydrate [SnCl₂·2H₂O, Aldrich] salts in distilled water. The overall solution concentration of copper and tin components was 0.5 M.

* Corresponding author. Tel.: +82 2 2049 6010; fax: +82 2 458 3504.
E-mail address: yckang@konkuk.ac.kr (Y.C. Kang).

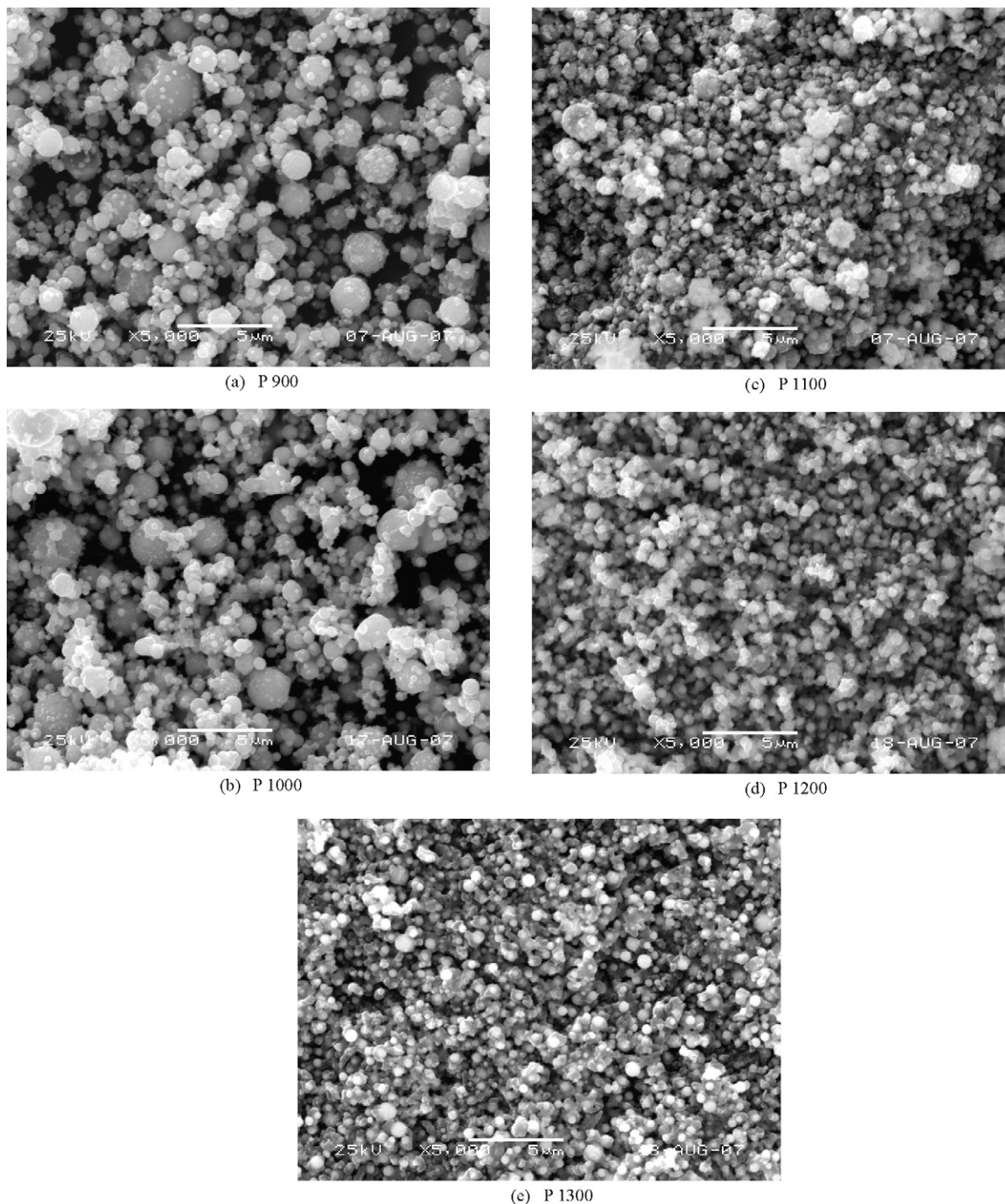


Fig. 1. SEM images of the Cu–Sn alloy powders prepared at different temperatures.

The crystal structures of the alloy powders were investigated using X-ray diffractometry (XRD, RIGAKU DMAX-33). The morphological characteristics of the alloy powders were investigated using scanning electron microscopy (SEM, JEOL JSM-6060) and a high-resolution transmission electron microscope (TEM, FEI, TECHNAI 300K). The capacities and cycle properties of the Cu–Sn alloy powders were measured by 2032-type coin cells. The electrode was made of 12 mg of Cu–Sn alloy powders mixed with 4 mg of a conductive binder (3.2 mg of teflonized acetylene black and 0.8 mg of graphite). The lithium metal and polypropylene film were used as the cathode electrode and the separator, respectively. The elec-

trolyte (TECHNO Semichem. Co.) was 1 M LiPF_6 in a 1:1 mixture by volume of EC/DMC. The entire cell was assembled in a glove box under an argon atmosphere. The charge/discharge characteristics of the samples were measured through cycling in the 0.1–1.5 V potential range at constant current densities of 0.1 C.

3. Results and discussion

The characteristics of the alloy powders prepared by spray pyrolysis were affected by the preparation temperatures. A high

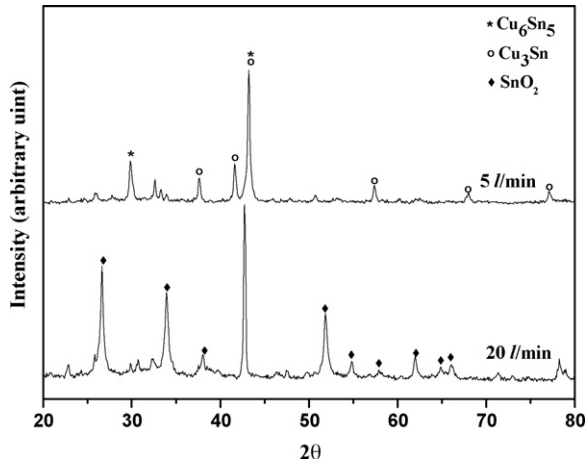


Fig. 2. XRD patterns of the Cu–Sn alloy powders prepared at different flow rates of the carrier gas.

enough preparation temperature was necessary to prepare the alloy powders with spherical shape, dense structure and fine size by reduction and melting processes. Fig. 1 shows the SEM images of the powders prepared at different temperatures. The flow rate of the carrier gas was 20 l min^{-1} . The prepared powders had spherical

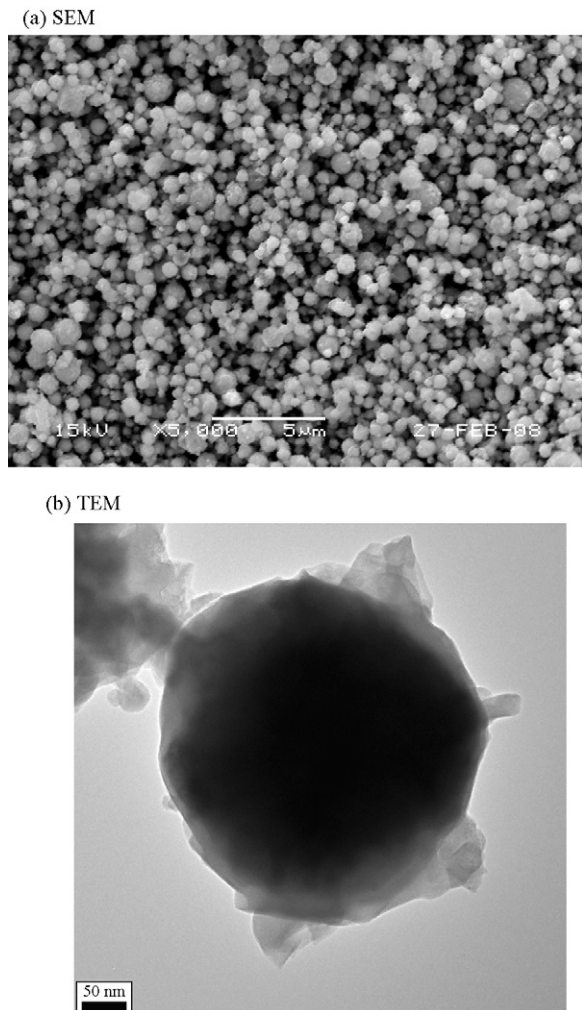


Fig. 3. SEM and TEM images of the Cu–Sn alloy powders.

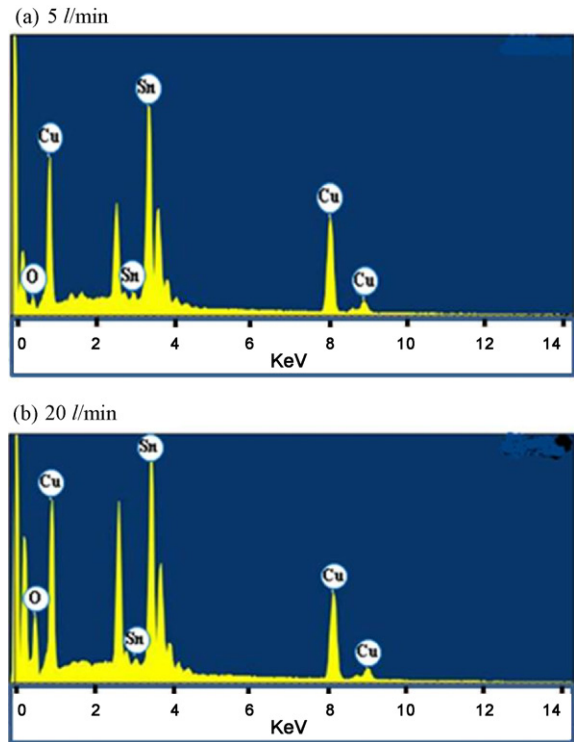


Fig. 4. EDAX spectra of the Cu–Sn alloy powders prepared at different flow rates of the carrier gas.

shape irrespective of the preparation temperatures. However, the mean sizes of the powders decreased with increasing the preparation temperatures. The mean sizes of the powders prepared at temperatures of 900 and 1300 °C were 1.5 and 0.7 μm. The powders prepared at a high temperature had narrower size distribution than the powders prepared at low temperature. The geometric standard deviations of the powders prepared at temperatures of 900 and 1300 °C were 1.9 and 1.2. The powders prepared at a low temperature of 900 °C had hollow inner structures, which could be estimated from the collapsed morphology of the powders as shown by arrows in Fig. 1(a). The size distributions of the powders prepared by spray pyrolysis could be changed by a change of the size distribution of droplets generated by the spray generator. The concentration gradient of precursors inside a large-sized droplet in the drying stage is higher than that inside a small-sized droplet. Therefore, the powders prepared at a low temperature of 900 °C from the large-sized droplets had a more hollow and porous structure than those prepared from the small-sized droplets. The different morphologies of the powders obtained from the small and large-sized droplets increased the size distribution of the powders prepared at a low temperature of 900 °C. However, melting of the alloy powders occurred at high temperatures above 1100 °C. Therefore, the powders prepared at high temperatures had dense inner structures and narrow size distributions. The XRD patterns of the powders prepared at low temperatures of 900 and 1000 °C had the main peaks of SnO₂ because of short residence time of the powders inside the hot wall reactor. The residence times of the powders inside the hot wall reactor were 1.2 and 1.1 s at preparation temperatures of 900 and 1000 °C. The XRD peak of metal phases appeared at a preparation temperature of 1000 °C. The peak intensities of metal phases increased with increasing the preparation temperatures. However, the XRD peaks of Cu₆Sn₅ alloy were not observed.

The residence time of the powders inside the hot wall reactor was increased by decreasing the flow rate of the carrier gas.

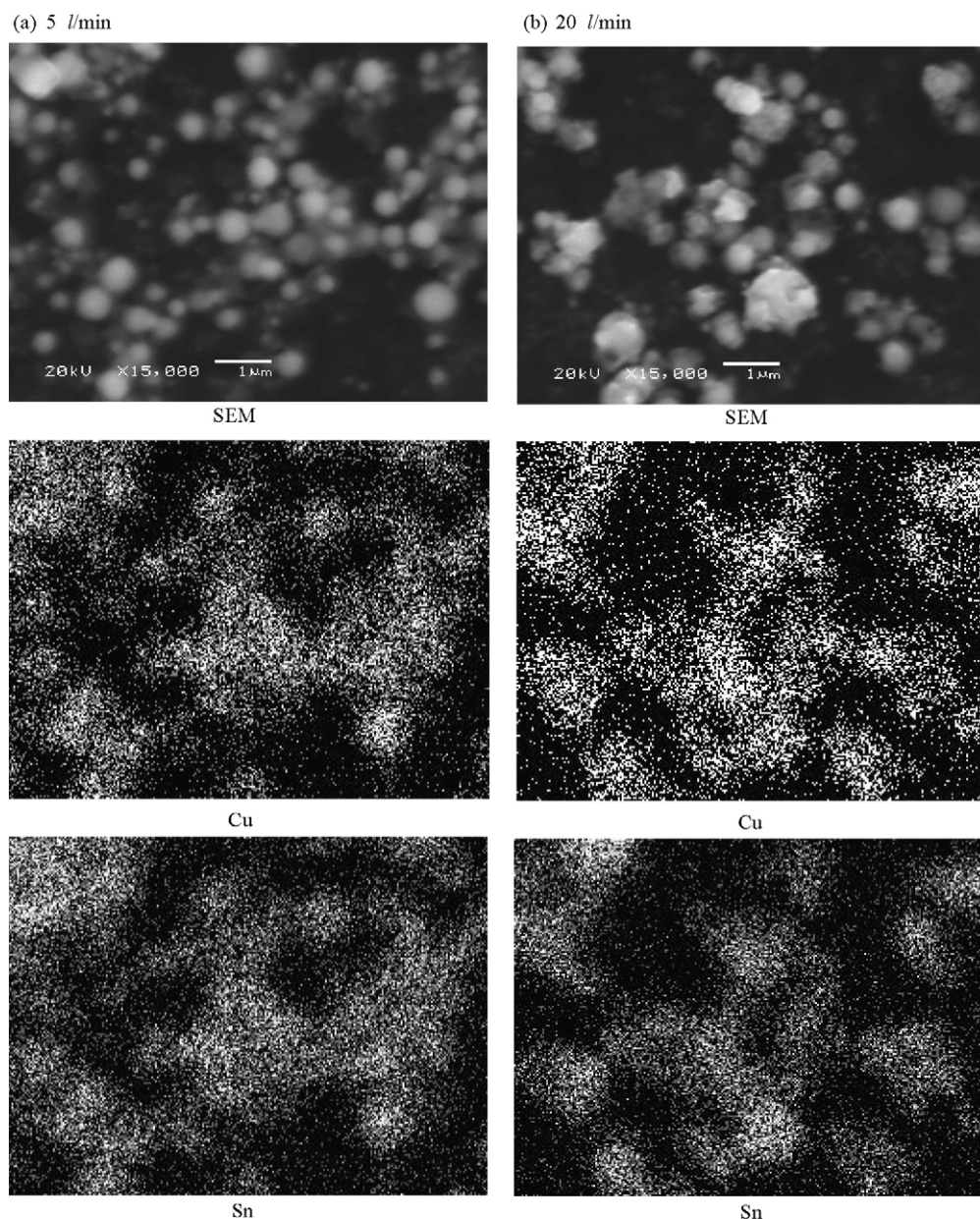


Fig. 5. Dot mappings of the Cu–Sn alloy powders prepared at different flow rates of the carrier gas.

Fig. 2 shows the XRD patterns of the powders prepared at a temperature of 1100 °C when the flow rates of the carrier gas were 5 and 20 l min⁻¹. The powders prepared at low flow rate of carrier gas as 5 l min⁻¹ had main XRD peaks of Cu₆Sn₅ alloy and copper-rich Cu₃Sn alloy phases. However, the powders prepared at high flow rate of carrier gas as 20 l min⁻¹ had main XRD peaks of SnO₂. Fig. 3 shows the SEM and TEM images of the alloy powders prepared by spray pyrolysis at a temperature of 1100 °C when the flow rate of the carrier gas was 5 l min⁻¹. The alloy powders had spherical morphology, dense inner structure and narrow size distribution.

Fig. 4 shows the EDAX spectra of the powders prepared at a temperature of 1100 °C when the flow rates of the carrier gas were 5 and 20 l min⁻¹. In the EDAX spectra, the composition ratios of the copper, tin and oxygen components were analyzed. The mole ratios of copper and tin components were well matched to that of the spray solution irrespective of flow rate of the carrier gas.

However, oxygen contents of the powders were strongly affected by the flow rate of the carrier gas. High intensity of the oxygen peak was detected from the EDAX spectrum of the powders prepared at high flow rate of carrier gas as 20 l min⁻¹. On the other hand, low intensity of the oxygen peak was detected from the EDAX spectrum of the powders prepared at high flow rate of carrier gas as 5 l min⁻¹. Fig. 5 shows the results of dot mapping of the Cu–Sn alloy powders prepared at a temperature of 1100 °C. Cu and Sn components were well dispersed inside the submicron-sized powders irrespective of the flow rate of the carrier gas. In the spray pyrolysis, alloy powders with homogeneous compositions could be prepared by micro-scale reaction within a droplet with submicron size.

The thermal analyses of the alloy powders prepared at a temperature of 1100 °C were shown in Fig. 6. In the TG curve, the total weight losses of the powders by evaporation of absorbed water and decomposition of residues below 400 °C were 3.76 and 8.71% when

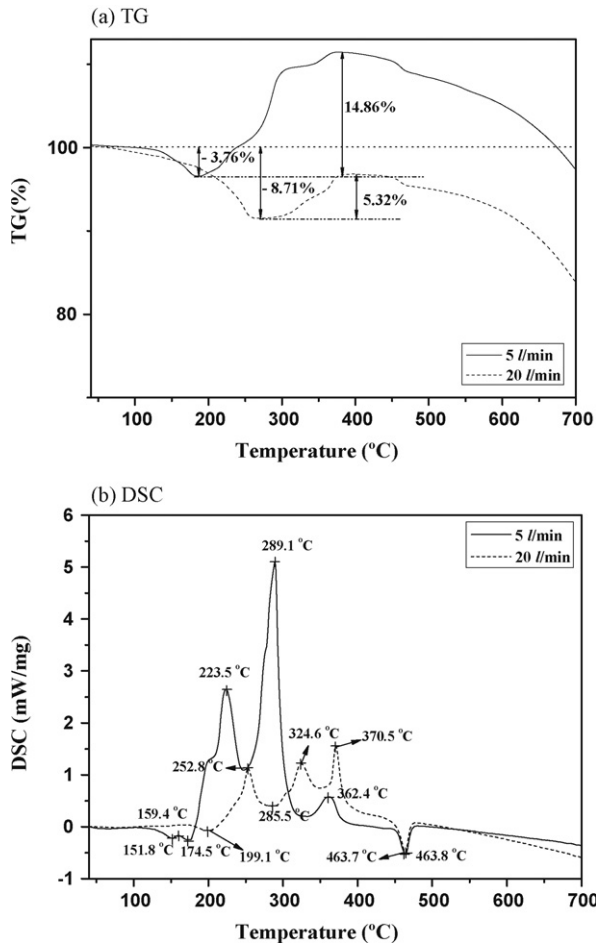


Fig. 6. TG/DSC curves of the Cu–Sn alloy powders prepared at different flow rates of the carrier gas.

the flow rates of the carrier gas were 5 and 201 min^{-1} . The weight increases due to the oxidation of the alloy powders in the range of temperatures between 185 and 400 $^{\circ}\text{C}$ were 14.86 and 5.32% when the flow rates of the carrier gas were 5 and 201 min^{-1} . The weight increase of the powders prepared at a flow rate of 201 min^{-1} was low because of low content of the alloy phases. In the DSC curves, the exothermic peaks due to the oxidation of the alloy powders were detected. The DSC curves had three exothermic peaks because of the prepared alloy powders had several phases. The locations of exothermic peaks moved to the high temperatures when the flow rate of carrier gas increased from 5 to 201 min^{-1} . The difference of alloy phases prepared at different flow rate of the carrier gas changed the locations of exothermic peaks.

Fig. 7 shows the initial charge/discharge curves of the Cu–Sn alloy powders prepared at different temperatures. The flow rate of the carrier gas was 201 min^{-1} . The initial charge and discharge capacities of the Cu–Sn alloy powders were affected by the preparation temperatures. The initial discharge capacities of the Cu–Sn alloy powders prepared at a temperature of 900, 1000 and 1100 $^{\circ}\text{C}$ were 436, 591 and 495 mAh g^{-1} . However, the alloy powders prepared at temperatures of 1200 and 1300 $^{\circ}\text{C}$ had very low discharge capacities of 154 and 160 mAh g^{-1} . The powders prepared at a temperature of 1100 $^{\circ}\text{C}$ had more good cycle properties than those prepared a temperature of 1000 $^{\circ}\text{C}$. The cycle properties of the Cu–Sn alloy powders prepared at a temperature of 1100 $^{\circ}\text{C}$ with different flow rate of the carrier gas were shown in Fig. 8. The Cu–Sn alloy powders had similar initial discharge capacities irrespective

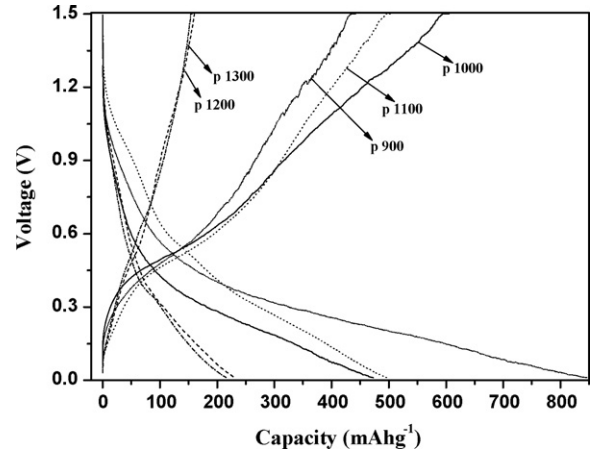


Fig. 7. Initial charge/discharge curves of the Cu–Sn alloy powders prepared at different temperatures.

of the flow rate of the carrier gas. However, the Cu–Sn alloy powders prepared at a low flow rate of 51 min^{-1} had more good cycle performance than those prepared at a high flow rate of 201 min^{-1} . The discharge capacities of the Cu–Sn alloy powders prepared at a flow rate of 51 min^{-1} dropped from 485 to 313 mAh g^{-1} by the 20th cycle at a current density of 0.1 C. On the other hand, the discharge capacities of the Cu–Sn alloy powder prepared at a flow rate

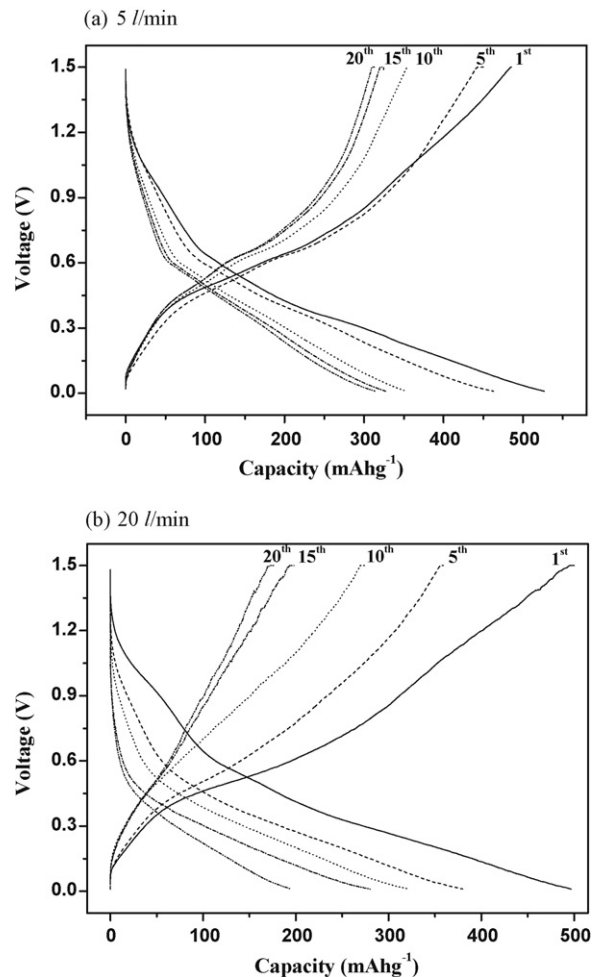


Fig. 8. Cycling performances of the Cu–Sn alloy powders prepared at different flow rate of the carrier gas.

of 201 min^{-1} dropped from 498 to 169 mAh g^{-1} by the 20th cycle at a current density of 0.1 C .

4. Conclusions

Cu–Sn alloy powders were directly prepared by spray pyrolysis at various preparation conditions. The preparation temperatures and flow rates of the carrier gas affected on the crystal structures, morphological and electrochemical properties of the alloy powders prepared by spray pyrolysis. The optimum preparation temperature to prepare the Cu–Sn alloy powders with fine size, spherical shape and high discharge capacities when the flow rate of the carrier gas of 5 l min^{-1} was 1100°C . The prepared Cu–Sn alloy powders with small amount of oxide impurities had homogeneous composition and crystal structures of Cu_6Sn_5 alloy and copper-rich Cu_3Sn alloy phases. The Cu–Sn alloy powders prepared at a low flow rate of 5 l min^{-1} had more good cycle performance than those prepared at a high flow rate of 20 l min^{-1} .

References

- [1] K.D. Kepler, J.T. Vaught, M.M. Thackeray, *Electrochem. Solid State Lett.* 2 (7) (1999) 307.
- [2] D. Larcher, L.Y. Besulien, D.D. MacNeil, J.R. Dahn, *J. Electrochem. Soc.* 147 (2000) 1658.
- [3] I.A. Courtney, J.R. Dahn, *J. Electrochem. Soc.* 144 (1997) 2045.
- [4] H.-C. Shin, M. Liu, *Adv. Funct. Mater.* 15 (4) (2005) 582.
- [5] L.B. Wang, S. Kitamura, K. Obata, *J. Power Sources* 141 (2) (2005) 286.
- [6] M. Valvo, U. Lafont, L. Simonin, E.M. Kelder, *J. Power Sources* 174 (2000) 428.
- [7] J. Yang, Y. Takeda, Q. Li, N. Imanishi, O. Yamamoto, *J. Power Sources* 90 (2000) 64.
- [8] F.S. Ke, L. Huang, H.H. Jiang, H.B. Wei, F.Z. Yang, S.G. Sun, *Electrochem. Commun.* 9 (2007) 228.
- [9] H. Mukaibo, T. Sumi, T. Yokoshima, T. Momma, T. Osaka, *Electrochem. Solid State Lett.* 6 (2003) A218.
- [10] G.X. Wang, L. Sun, D.H. Bradhurst, *J. Alloy Compd.* 299 (2000) L12.
- [11] D.G. Kim, H. Kim, H.J. Sohn, *J. Power Sources* 104 (2002) 221.
- [12] J. Wolfenstine, S. Campos, D. Foster, *J. Power Sources* 109 (2002) 230.
- [13] C.H. Mi, X.G. Zhang, G.S. Cao, *J. Inorg. Mater.* 19 (2003) 283.
- [14] S. Gürmen, S. Stopić, B. Friedrich, *Mater. Res. Bull.* 41 (2006) 1882.
- [15] K. Nagashima, M. Wada, A. Kato, *J. Mater. Res.* 5 (1990) 2828.